

Hydrothermal synthesis and structures of the novel niobium phosphates $\text{Ba}_2[\text{NbOF}(\text{PO}_4)_2]$ and $\text{Ba}_3[\text{Nb}_3\text{O}_3\text{F}(\text{PO}_4)_4(\text{HPO}_4)](\text{H}_2\text{O})_7$

Xiqu Wang,* Lumei Liu and Allan J. Jacobson

Department of Chemistry and Materials Research Science and Engineering Center, University of Houston, Houston, Texas, 77204-5003, USA. E-mail: xiqu.wang@mail.uh.edu; Fax: 713-7432787; Tel: 713-7432780

Received 15th February 2002, Accepted 28th March 2002

First published as an Advance Article on the web 18th April 2002

The new niobium phosphates $\text{Ba}_2[\text{NbOF}(\text{PO}_4)_2]$ (**1**) and $\text{Ba}_3[\text{Nb}_3\text{O}_3\text{F}(\text{PO}_4)_4(\text{HPO}_4)](\text{H}_2\text{O})_7$ (**2**) have been synthesized in single crystal form by hydrothermal reactions at mild temperatures. Their crystal structures determined from X-ray diffraction data are based on defected derivatives of the $\text{NbO}(\text{H}_2\text{O})\text{PO}_4$ layers found in hydrated niobium phosphate. The niobium phosphate layers in **1** or **2** can be derived by removing one half or one quarter of the NbO_6 octahedra from the $\text{NbO}(\text{H}_2\text{O})\text{PO}_4$ layer, respectively. In compound **1** the layers are separated and are held together by interlayer Ba-O and Ba-F bonds while in **2** the layers are linked by interlayer PO_4 tetrahedra to form a framework structure.

Introduction

Crystalline niobium phosphates are of interest because they have potential applications in diverse areas such as luminescence,^{1,2} nonlinear optical materials,³ ion-exchange and heterogeneous catalysis.⁴⁻⁸ In contrast to the large number of vanadium phosphates which are structurally based on the VOPO_4 layers of $\text{VOPO}_4 \cdot 2\text{H}_2\text{O}$, only a few corresponding niobium phosphates have been reported. Hydrated niobium phosphate, $\text{NbOPO}_4 \cdot n\text{H}_2\text{O}$, consists of layers of composition $\text{NbO}(\text{H}_2\text{O})\text{PO}_4$ in which NbO_6 distorted octahedra are connected in their equatorial planes by PO_4 tetrahedra *via* sharing corners. Various types of amines and alcohols can be intercalated between the formally electroneutral $\text{NbO}(\text{H}_2\text{O})\text{PO}_4$ layers.⁴ The intercalation chemistry is similar to that first observed in $\text{VOPO}_4 \cdot 2\text{H}_2\text{O}$. In $\text{Nb}_2(\text{OH})_2(\text{HPO}_4)(\text{PO}_4)_2 \cdot n\text{H}_2\text{O}$ and $\text{ANb}_2(\text{OH})_2(\text{PO}_4)_3 \cdot n\text{H}_2\text{O}$, A = Na, K, the niobyl phosphate layers are believed to be connected by interlayer PO_4 tetrahedra to form 3-dimensional frameworks.⁵ The extra-framework monovalent cations are known to be exchangeable with other alkali-, alkaline-earth-metal and alkylammonium ions. However, no accurate structure data are available for these niobium phosphate phases. Similar structures are known and well characterized for vanadium phosphates.⁹⁻¹¹

In our hydrothermal synthesis studies, a number of known and new niobium phosphates have been obtained in single crystal form,^{12,13} including $[(\text{NbOPO}_4)_4(\text{H}_3\text{NCH}_2\text{COOH})_2][\text{H}_2\text{PO}_4][\text{OH}, \text{F}]$ that contains glycinium cations bridging the NbOPO_4 layers.¹⁴ The crystal structures of most of these new compounds were determined from single crystal X-ray data. Some of them are promising new materials for ion-exchange and intercalation reactions. Here we report the synthesis and structures of two novel barium niobium phosphates $\text{Ba}_2[\text{NbOF}(\text{PO}_4)_2]$ (**1**) and $\text{Ba}_3[\text{Nb}_3\text{O}_3\text{F}(\text{PO}_4)_4(\text{HPO}_4)](\text{H}_2\text{O})_7$ (**2**). The structures of **1** and **2** are based on defect $\text{NbO}(\text{H}_2\text{O})\text{PO}_4$ layers.

Experimental

Synthesis

For the synthesis of compound **1**, a solution prepared by mixing 0.17 ml 85% phosphoric acid (EM Science), 33 mg

NH_4HF_2 (99.999%, Aldrich) and 2 ml H_2O was sealed together with 231 mg $\text{Ba}(\text{OH})_2 \cdot 8\text{H}_2\text{O}$ (98%, Aldrich), 14 mg Nd_2O_3 (99.99%, Aldrich) and 15 mg niobium metal (99.8%, Aldrich) in a flexible Teflon bag in air. The bag was then placed in a RENE41 reaction vessel of a Leco HR-1B-2 high pressure/high temperature system, and heated at 260 °C under an applied pressure of 120 MPa for 22 h. Colorless plates of **1** formed on the surface of unreacted niobium metal. The yield is about 20% based on Nb. No detectable Nd was found in the crystals of **1** by electron microprobe analysis. Nd_2O_3 was used in the synthesis aiming at a new compound containing neodymium. Its role in the formation of **1** is not clear.

Compound **2** was synthesized by using a 23 ml Teflon lined autoclave. The starting reagent that contains 0.17 ml 85% phosphoric acid, 33 mg NH_4HF_2 , 2 ml H_2O , 231 mg $\text{Ba}(\text{OH})_2 \cdot 8\text{H}_2\text{O}$ and 15 mg niobium metal, was heated first at 160 °C for 2 days and then at 200 °C for 3 days. Colorless prisms of **2** formed on the surface of unreacted niobium metal together with plates of the impurity phase BaHPO_4 . The yield is about 10% based on Nb. Efforts to improve the yield and eliminate the impurities by changing the starting composition and temperature were unsuccessful.

Characterization

Chemical compositions were analyzed using a JEOL 8600 electron microprobe operating at 15 KeV with a 10 μm beam diameter and a beam current of 30 nA. The measured atomic ratios Ba : Nb : P : F = 2.0 : 1.0 : 2.0 : 0.7 for **1** and Ba : Nb : P : F = 3.0 : 2.8 : 4.9 : 1.0 for **2** are consistent with the title formulae derived from the structure refinements.

Thermogravimetric analysis for **2** was carried out on a DuPont 2100 TGA system with a heating rate of 5 °C min^{-1} in air after initially equilibrating the sample at 50 °C for 20 min to remove any surface water. A sharp weight loss of 6.8% corresponding to $\sim 5 \text{H}_2\text{O}$ per formula unit was observed between 100–260 °C. A subsequent gradual weight loss of a further 2.8% began at ca. 260 °C and was completed at ca. 600 °C. The total weight loss of 9.6% observed below 600 °C corresponds to 7.3 H_2O per formula unit.

Single crystal X-ray data were measured on a SMART platform diffractometer equipped with a 1 K CCD area detector using graphite-monochromatized $\text{MoK}\alpha$ radiation at

Table 1 Crystal data and structure refinement details

	1	2
Formula	Ba ₂ FNbO ₉ P ₂	H ₁₄ Ba ₃ FNb ₃ O ₃₀ P ₅
F. W.	592.5	1358.7
Temperature/K	293(2)	293(2)
Wavelength/Å	0.71073	0.71073
Space group	<i>P2₁/c</i>	<i>I mmm</i>
<i>a</i> /Å	7.0570(7)	9.4824(6)
<i>b</i> /Å	7.1618(8)	15.0067(9)
<i>c</i> /Å	9.0246(9)	18.490(1)
β /°	91.09(1)	90
<i>V</i> /Å ³	456.03(8)	2631.1(3)
<i>Z</i>	2	4
Absorption coefficient/mm ⁻¹	10.2	6.1
θ_{\max} /°	24.8	28.6
Reflections collected	2235	8275
Independent reflections	779	1786
<i>R</i> (int)	0.0270	0.0385
Data/parameters	779/74	1786/151
Goodness-of-fit	1.224	1.077
<i>R1</i> / <i>wR2</i> [<i>I</i> > 2σ(<i>I</i>)]	0.0186/0.0439	0.0402/0.1003
<i>R1</i> / <i>wR2</i> (all data)	0.0190/0.0441	0.0488/0.1042
Extinction coefficient	0.0044(4)	0.00044(9)
Max. diff. peak/hole/e Å ⁻³	0.62/-0.62	1.38/-1.98
<i>R1</i> = $\sum F_o - F_c /\sum F_o $, <i>wR2</i> = $[\sum(w(F_o^2 - F_c^2)^2)/\sum(wF_o^2)^2]^{1/2}$.		

293 K. For each phase a hemisphere of data (1271 frames at 5 cm detector distance) was collected using a narrow-frame method with scan widths of 0.30° in ω and an exposure time of 30 s frame⁻¹. The data were integrated using the Siemens SAINT program.¹⁵ Absorption correction was made using the program SADABS.¹⁶ The structures were solved by direct methods and refined using SHELXTL.¹⁷ For compound **2**, some Ba cations, water oxygen atoms and phosphate groups were found to be highly disordered with fractional occupancies. Constraints for the total Ba and P contents were applied in order to refine relative occupancies of each site. Soft constraints for the bond lengths of the disordered PO₄ groups were also applied. Structure refinements for **2** located 6.6 H₂O per formula unit which is slightly less than that observed by thermogravimetric analysis. Part of the disordered water molecules might not be located in the refinements because of overlapping electron density with the disordered Ba cations and phosphate groups. Crystallographic and refinement details are summarized in Table 1. Table 2 and Table 3 list selected bond lengths.†

Structure description and discussion

The structure of Ba₂[(NbOF)(PO₄)₂] (1)

Fig. 1 shows the coordination environments of the cations in **1**. The five oxygen and one fluorine atoms bonding to the niobium atom form a quite regular octahedron, but the Nb atom is displaced from the center to one oxygen corner (O2) leading to a short niobyl Nb=O bond (1.77 Å) and a long Nb–F bond (2.09 Å) in *trans* positions. The other four equatorial Nb–O bond lengths are between 1.98 and 2.05 Å. The NbO₅F octahedron is found randomly disordered over two orientations with opposite apical Nb=O bonds. Each NbO₅F octahedron is connected with four PO₄ tetrahedra by sharing common corners, with Nb–O–P bond angles ranging from 133.5–146.2°. Neighboring octahedra are bridged by a PO₄ tetrahedron in the equatorial plane to form an infinite layer with composition (NbOF)(PO₄)₂. The layers are stacked along the *a* axis and are held together by interlayer Ba–O and Ba–F bonds (Fig. 2). The interlayer barium cation has a coordination number of 9 with Ba–(O,F) bond lengths of 2.64–3.09 Å.

†CCDC reference numbers 179664 and 179665. See <http://www.rsc.org/suppdata/jm/b2/b201701f/> for crystallographic files in .cif or other electronic format.

Table 2 Selected bond lengths (Å) for **1**

Nb–O(2)	1.772(8)	Ba–O(1)	2.641(3)
Nb–O(4)	1.98(2)	Ba–O(2),F	2.720(3)
Nb–O(5)	1.99(2)	Ba–O(1)	2.740(3)
Nb–O(4)	2.00(2)	Ba–O(3)	2.765(3)
Nb–O(5)	2.05(2)	Ba–O(2),F	2.811(3)
Nb–F	2.087(9)	Ba–O(4)	2.850(3)
		Ba–O(3)	2.894(3)
P–O(1)	1.512(3)	Ba–O(5)	3.048(3)
P–O(3)	1.515(4)	Ba–O(3)	3.091(3)
P–O(5)	1.563(3)		
P–O(4)	1.572(3)		

Table 3 Selected bond lengths (Å) for **2**

Nb(1)–O(2)	1.906(9)	P(2A)–O(9A)	1.511(9)
Nb(1)–F	1.944(12)	P(2A)–O(8B)	1.524(10)
Nb(1)–O(3) × 4	1.974(4)	P(2A)–O(7) × 2	1.533(6)
Nb(2)–O(5)	1.722(6)	P(2A)–O(8A)	1.523(10)
Nb(2)–O(1) × 2	2.014(4)	P(2A)–O(9B)	1.533(10)
Nb(2)–O(4) × 2	2.020(4)	P(2A)–O(7) × 2	1.533(6)
Nb(2)–O(7)	2.180(6)		
P(1)–O(6)	1.488(4)	P(2B)–O(7) × 2	1.525(9)
P(1)–O(1)	1.538(4)	P(2B)–O(9A) × 2	1.534(10)
P(1)–O(4)	1.545(4)		
P(1)–O(3)	1.557(5)		

Refinements of low symmetry structure models with ordered NbO₅F octahedra were unsuccessful.

The structure of Ba₃[Nb₃O₃F(PO₄)₄](HPO₄)](H₂O)₇ (2)

In the structure of **2**, niobium phosphate layers are linked into a framework structure by interlayer phosphate tetrahedra. Fig. 3 shows the coordination environments of the framework cations. The Nb(1) atom is coordinated to five oxygen atoms and a fluorine atom in an octahedral configuration. Noticeable elongation of the thermal ellipsoids of the Nb(1) and other atom positions (F, O3 in particular) indicates possible orientational disorder of the Nb(1)O₅F octahedra similar to that found in compound **1**. However, refinements of the models incorporating such disorder were unsuccessful. The Nb(2) atom has an octahedral coordination with a Nb=O bond of 1.72 Å and a long Nb–O bond of 2.18 Å along the apical axis. The four equatorial Nb–O bonds are 2.01–2.02 Å, slightly longer than those of Nb(1) (1.97 Å).

Neighboring Nb(2)O₆ octahedra are bridged by two P(1)O₄

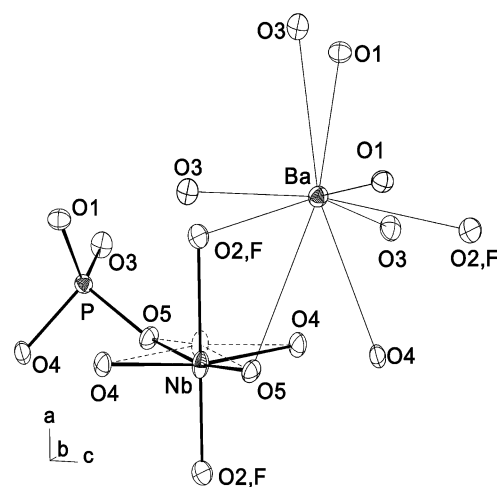


Fig. 1 Coordination environments of cations in **1**. Thermal ellipsoids are at 50% probability. The NbO₅F octahedron is randomly disordered over two orientations, one of which is shown with dashed lines.

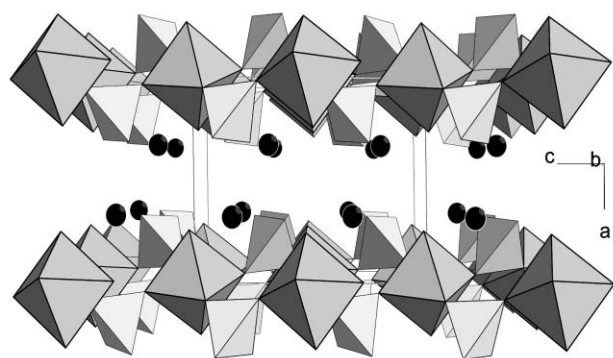
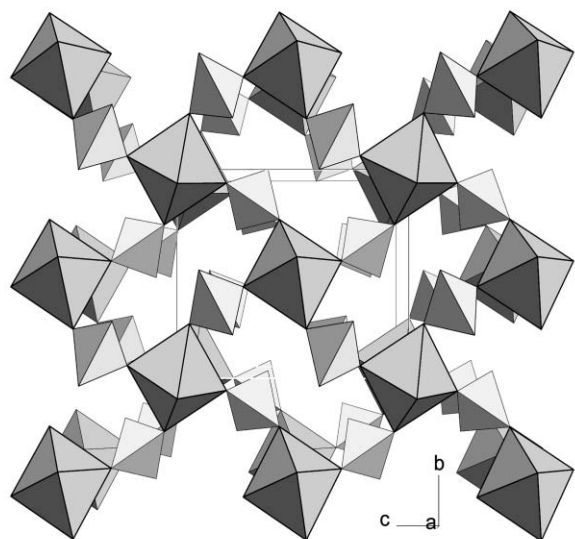


Fig. 2 Views of the structure of **1** along *a* (top) and *b* axis (bottom). Black circles represent Ba atom positions.

tetrahedra in the equatorial plane to form an infinite chain of composition $\text{NbO}_2(\text{PO}_4)_2$ running along [100]. The chains are cross-linked by the $\text{Nb}(1)\text{O}_5\text{F}$ octahedra to form a (010) layer of composition $\text{Nb}_3\text{O}_5\text{F}(\text{PO}_4)_4$ (Fig. 4). Each $\text{P}(1)\text{O}_4$

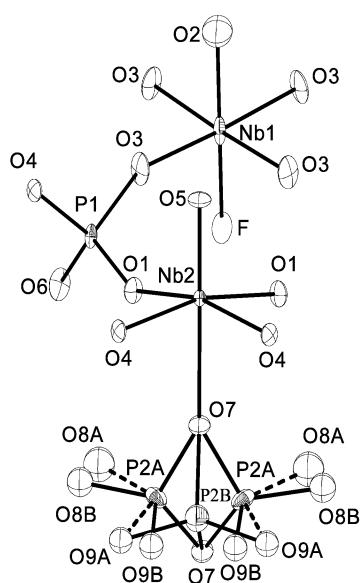


Fig. 3 Coordination environments of framework cations in **2**. Thermal ellipsoids are at 50% probability. The $\text{P}(2)\text{O}_4$ tetrahedra are disordered over five different orientations.

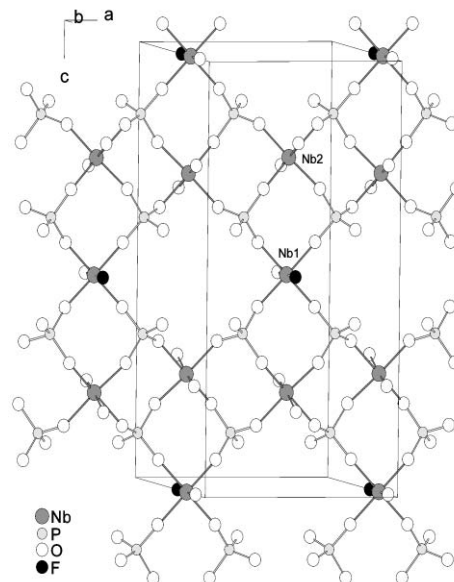


Fig. 4 Ball-and-stick representation of the $\text{Nb}_3\text{O}_5\text{F}(\text{PO}_4)_4$ layer of **2**.

tetrahedron is connected with two $\text{Nb}(2)\text{O}_6$ octahedra and one $\text{Nb}(1)\text{O}_5\text{F}$ octahedron by sharing corners, with Nb–O–P bond angles in the range 134.4–151.7°. The fourth corner of the $\text{P}(1)\text{O}_4$ tetrahedron is terminal. The layers are stacked along the [010] direction. Neighboring layers are related by a mirror plane and are cross-linked by the $\text{P}(2)\text{O}_4$ tetrahedra that share corners with two $\text{Nb}(2)\text{O}_6$ octahedra from neighboring layers. The interlayer $\text{P}(2)\text{O}_4$ tetrahedra are disordered among five different orientations (Fig. 3, 5). The barium cations and water molecules are located between the layers. Both are highly disordered with small fractional occupancies. Ba(1–4) have well-defined coordination spheres consisting of framework and water oxygen atoms. An incomplete coordination environment is found for Ba(5) probably because some disordered water molecules could not be located. Ba(5) has the lowest site occupancy and cannot be unambiguously distinguished from disordered water oxygen atoms.

Relations to other known structures

In the $\text{NbO}(\text{H}_2\text{O})\text{PO}_4$ layer of the hydrated niobium phosphate $\text{NbOPO}_4 \cdot n\text{H}_2\text{O}$ each PO_4 tetrahedron is connected with four NbO_6 octahedra and each NbO_6 octahedron is connected with four PO_4 tetrahedra in its equatorial plane *via* sharing corners. If one half of the octahedra are removed from the $\text{NbO}(\text{H}_2\text{O})\text{PO}_4$ layer so that two corners of the bridging PO_4 tetrahedra are terminal, the resulting layer will be structurally the same as the $\text{NbOF}(\text{PO}_4)_2$ layer of **1**. If one quarter of the octahedra are removed from the $\text{NbO}(\text{H}_2\text{O})\text{PO}_4$ layer so that one corner of the bridging PO_4 tetrahedra is terminal, the resulting layer will be structurally the same as the $\text{Nb}_3\text{O}_5\text{F}(\text{PO}_4)_4$ layer of **2**.

Topologically the $\text{NbOF}(\text{PO}_4)_2$ layer of **1** is equivalent to the layer of $\text{VO}(\text{H}_2\text{PO}_4)_2$ ¹⁸ and the $\text{Fe}(\text{H}_2\text{O})_2(\text{SO}_4)_2$ layer of the mineral rhomboclase $(\text{H}_5\text{O}_2)\text{Fe}(\text{H}_2\text{O})_2(\text{SO}_4)_2$ where the Fe^{3+}O_6 octahedron has two terminal water oxygen corners.¹⁹ In $\text{VO}(\text{H}_2\text{PO}_4)_2$ the layers are cross-linked by O–V–O–V=O bonds. The mineral olmsteadite $\text{KF}_2[\text{NbO}_2(\text{PO}_4)_2](\text{H}_2\text{O})_2$ ²⁰ contains $\text{NbO}_2(\text{PO}_4)_2$ layers again closely related to that of **1**. The major difference between the two layers is that the two terminal corners of the niobium octahedra are in *cis* positions in olmsteadite instead of in *trans* positions as in **1**.

The synthetic compound $(\text{H}_2\text{NC}_4\text{H}_8\text{NH}_2)_2[(\text{VO})_3(\text{HPO}_4)_2(\text{PO}_4)_2](\text{H}_2\text{O})$ ²¹ (**3**) has a layered structure with vanadium phosphate layers similar to the niobium phosphate layer of **2**. The vanadium phosphate layers of **3** can also be derived

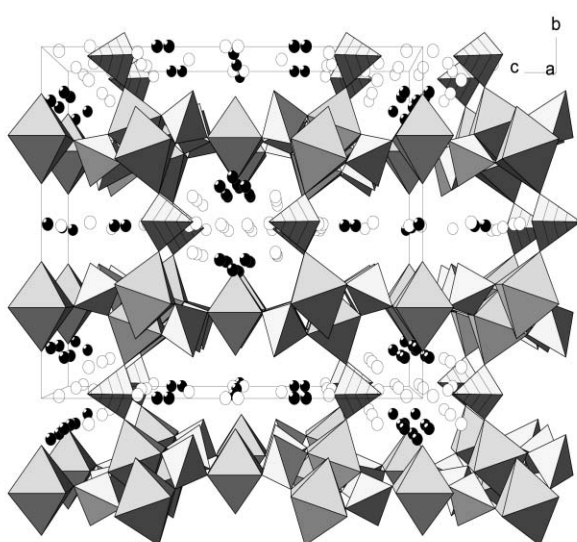
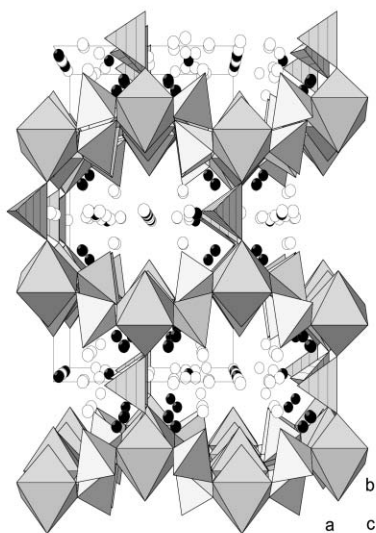


Fig. 5 Views of the structure of **2** along *c* (top) and *a* axis (bottom). Only one orientation of the interlayer $P(2)O_4$ tetrahedra is plotted and marked by hatching. Open and solid circles represent water oxygen and barium atom positions respectively.

by removing one quarter of the octahedra from the $NbO(H_2O)PO_4$ layer in a similar way as for the layers of **2**. In the layers of **3**, however, one third of the remaining octahedra are replaced by VO_5 tetragonal pyramids and each of the remaining VO_6 octahedra shares an edge with a PO_4 tetrahedron, thus only a half of the PO_4 tetrahedra have a terminal oxygen corner. The lower valence of V^{4+} compared to Nb^{5+} may be a necessary factor for the occurrence of edge-sharing between the PO_4 tetrahedra and the VO_6 octahedra. This edge-sharing linkage effectively prevents interlayer connection by further phosphate groups in **3** because, except for terminal oxygen of $V=O$ bonds, all the oxygen atoms in the layer are bonded to a V^{4+} and a P^{5+} cation. A large family of framework structures formed from $MOXO_4$ layers that are bridged by XO_4 tetrahedra are well known.^{9–11} Compound **2** represents an example of forming open framework structures by bridging defect $MOXO_4$ layers.

Conclusions

Hydrothermal reactions at mild temperatures resulted in the new niobium phosphates **1** and **2** in single crystal form. Both compounds contain defected $NbO(H_2O)PO_4$ layers. If in an ideal case the fluorine atoms in compound **1** are all located on one side of the layer in an ordered fashion, a strongly polar layered structure will be obtained which may have interesting optical and chemical properties. Intercalation of proper interlayer species such as alkylammonium cations during synthesis may help the ordering, *e.g.*, through hydrogen bonding. Compound **2** is closely related to the known compounds $ANb_2(OH)_2(PO_4)_3 \cdot nH_2O$, $A = Na, K$, that are based on non-defected $NbO(H_2O)PO_4$ layers. As the latter exhibit well defined ion-exchange properties, similar properties are expected for compound **2**.

Acknowledgement

We thank the National Science Foundation (DMR9805881) and the R. A. Welch Foundation for financial support. This work made use of MRSEC/TCSUH Shared Experimental Facilities supported by the National Science Foundation under Award Number DMR-9632667 and the Texas Center for Superconductivity at the University of Houston.

References

- 1 G. Blasse, G. J. Dirksen, M. F. Hazenkamp, A. Verbaere and S. Oyetola, *Eur. J. Solid State Chem.*, 1989, **26**, 175.
- 2 M. F. Hazenkamp, G. Blasse, J. J. Zah-Letho and A. Verbaere, *Eur. J. Solid State Chem.*, 1992, **29**, 1263.
- 3 C. S. Liang, W. T. A. Harrison, M. M. Eddy, T. E. Gier and G. Stucky, *Chem. Mater.*, 1993, **5**, 917.
- 4 K. Beneke and G. Lagaly, *Inorg. Chem.*, 1983, **22**, 1503.
- 5 N. Kinomura and N. Kumada, *Inorg. Chem.*, 1990, **29**, 5217.
- 6 Y.-K. Shin and D. G. Nocera, *J. Am. Chem. Soc.*, 1992, **114**, 1264.
- 7 K. Tanabe and S. Okazaki, *Appl. Catal., A*, 1995, **133**, 191.
- 8 I. Nowak and M. Ziolk, *Chem. Rev.*, 1999, **99**, 3603.
- 9 W. T. Harrison, K. Hsu and A. J. Jacobson, *Chem. Mater.*, 1995, **7**, 2004.
- 10 M. Schindler, W. Joswig and W. H. Baur, *J. Solid State Chem.*, 1999, **145**, 15.
- 11 J. Do, R. Bontchev and A. J. Jacobson, *J. Solid State Chem.*, 2000, **154**, 514.
- 12 X. Wang, L. Liu, H. Cheng, K. Ross and A. J. Jacobson, *J. Mater. Chem.*, 2000, **10**, 1203.
- 13 X. Wang, L. Liu and A. J. Jacobson, *J. Mater. Chem.*, 2000, **10**, 2774.
- 14 X. Wang, L. Liu, H. Cheng and A. J. Jacobson, *Chem. Commun.*, 1999, 2531.
- 15 SAINT, Program for Data Extraction and Reduction, Siemens Analytical X-ray Instruments Inc., Madison, USA, 1996.
- 16 G. M. Sheldrick, SADABS, Program for Siemens Area Detector Absorption Corrections, University of Gottingen, Germany, 1997.
- 17 G. M. Sheldrick, SHELXTL, Program for Refinement of Crystal Structures, Siemens Analytical X-ray Instruments Inc., Madison, USA, 1994.
- 18 S. A. Linde, Y. E. Gorbunova, A. V. Lavrov and V. G. Kuznetsov, *Dokl. Akad. Nauk SSSR*, 1979, **244**, 1411.
- 19 K. Mereiter, *Tschermaks Mineral. Petrogr. Mitt.*, 1974, **21**, 216.
- 20 P. B. Moore, T. Araki, A. R. Kampf and M. Steele, *Am. Mineral.*, 1976, **61**, 5.
- 21 V. Soghomonian, R. C. Haushalter, Q. Chen and J. Zubieta, *Inorg. Chem.*, 1994, **33**, 1700.